Huang, S. Y., Sahraoui, F., Yuan, Z. G., Contel, O. L., Breuillard, H., He, J. S., Zhao, J. S., Fu, H. S., Zhou, M., Deng, X. H., Wang, D., Du, J. W., Yu, X. D., Wang, D. D., Pollock, C. J., Torbert, R. B., Burch, J. L. (2018): Observations of Whistler Waves Correlated with Electron-scale Coherent Structures in the Magnetosheath Turbulent Plasma. - *The Astrophysical Journal*, *861*, 1.

DOI: http://doi.org/10.3847/1538-4357/aac831

Observations of whistler waves correlated with electron-scale coherent structures in the magnetosheath turbulent plasma

S. Y. Huang[1], F. Sahraoui[2], Z. G. Yuan[1], O. Le Contel[2], H. Breuillard[2], J. S. He[3], J. S. Zhao[4], H. S. Fu[5], M. Zhou[6], X. H. Deng[6], X. Y. Wang[1], J. W. Du[1], X. D. Yu[1], D. D. Wang[1,7], C. J. Pollock[8], R. B. Torbert[9], and J. L. Burch[10]

[1]School of Electronic Information, Wuhan University, Wuhan, China

[2]Laboratoire de Physique des Plasmas, CNRS-Ecole Polytechnique-UPMC, Palaiseau, France

[3]School of Earth and Space Sciences, Peking University, Beijing, China

[4]Key Laboratory of Planetary Sciences, Purple Mountain Observatory, Chinese Academy of Sciences, Nanjing, China

[5]School of Space and Environment, Beihang University, Beijing, China

[6]Institute of Space Science and Technology, Nanchang University, Nanchang, China

[7]Helmholtz Centre Potsdam GFZ German Research Centre for Geosciences, Germany

[8]NASA, Goddard Space Flight Center, Greenbelt, Maryland, USA

[9] Physics Department, University of New Hampshire, Durham, New Hampshire, USA

[10]Southwest Research Institute, San Antonio TX, USA

Abstract

A new type of electron-scale coherent structure, referred to as electron vortex magnetic holes, was identified recently in the Earth's magnetosheath turbulent plasma. These electron-scale magnetic holes are characterized by magnetic field strength depression, electron density enhancement, temperature and temperature anisotropy increase (significant increase in perpendicular temperature and decrease in parallel temperature), and an electron vortex formed by the trapped electrons. The strong increase of electron temperature indicates that these magnetic holes have strong connection with the energization of electrons. Here, using high time resolution *in-situ* measurements from the MMS mission, it is further shown that electron-scale whistler waves coexist with electron-scale magnetic holes. These whistler waves were found

not propagating from remote regions, but generated locally due to electron temperature anisotropy ($T_{e\perp}/T_{e\parallel}$) inside the magnetic holes. This study provides new insights into the electron-scale plasma dynamics in turbulent plasmas.

1. Introduction

Magnetic holes, characterized by magnetic field strength depressions lasting from several seconds to several minutes (corresponding to a spatial scale larger than ion gyro-radius), have been detected in space plasmas such as the magnetosphere (e.g. Shi et al. 2009; Sundberg et al. 2015), magnetosheath (e.g. Tsurutani et al. 2011) or the solar wind (e.g. Tsurutani et al. 2002; Zhang et al. 2008). These large-scale magnetic holes are thought to be generated by mirror instability (Horbury et al. 2004; Sahraoui et al., 2004, 2006) or related to slow solitons (Stasiewicz, 2004). Recently, thanks to the unprecedented high time resolution data of MMS mission, a new type of kinetic-size magnetic holes (less than proton gyro-radius, or tens of electron gyro-radius) was evidenced in the turbulent magnetosheath plasma (Huang et al. 2017a, 2017b; Yao et al. 2017). A statistical study showed that an increase in the electron density and total temperature, significantly increase (resp. slightly decrease) in the electron perpendicular (resp. parallel) temperature (Huang et al. 2017b). Furthermore, an electron vortex is formed by the trapped electrons with enhanced fluxes at ~90° pitch angles inside the magnetic holes (Huang et al. 2017b). The increase of electron temperature inside the magnetic holes suggests the possible role the latter could play in energy dissipation in turbulent plasmas leading to localized electron heating (Breuillard et al. 2016a; Huang et al. 2012a, 2014, 2017d; Fu et al. 2017). These magnetic holes can be best interpreted as electron vortex magnetic holes according to Particle-In-Cell (PIC) simulations of Haynes et al. (2015).

Whistler waves are frequently reported in space and laboratory plasmas (Stenzel, 1999), such as the inner magnetosphere (e.g. Li et al. 2011; Fu et al. 2012, 2014), the magnetotail (e.g. Huang et al. 2010, 2012b, 2016a, 2017c; Zhima et al. 2015; Breuillard et al. 2016b), the magnetosheath (e.g. Moullard et al. 2002; Breuillard et al. 2017, Huang et al. 2016b; Cao et al.

2017), and the solar wind (e.g. Lacombe et al. 2014). They can be generated by various mechanisms that include electron temperature anisotropies (e.g. Gary and Madland, 1985) and current or beam-driven instabilities (e.g., Zhang et al. 1999; Fujimoto et al. 2014). Whistler waves propagating in the magnetosphere (Santolik et al. 2009; Breuillard et al. 2012, 2014) can be guided by density enhancements or depletions (e.g., Smith et al. 1961; Moullard et al. 2002; Streltsov et al. 2006; Li et al. 2011) and modulated by ULF waves (e.g. Xia et al. 2016). The occurrence of whistler waves is generally well correlated with the existence of magnetic structures with magnetic field strength minimum (Smith and Tsurutani, 1976; Dubinin et al. 2007) or dipolarization fronts (Le Contel et al. 2009; Deng et al. 2010; Huang et al. 2012b; Li et al. 2015). Recently, Tenerani et al. (2012, 2013) have reported the connection between whistler waves and ion-scale magnetic structures using Cluster measurements in the magnetotail.

However, whether whistler waves can correlate with electron-scale coherent magnetic structures are still unsettled. In this Letter, we report observations of intense whistler waves correlated with electron-scale magnetic holes (i.e., electron vortex magnetic holes) in the turbulent magnetosheath plasma from the MMS spacecraft. The magnetic field data come from the Fluxgate Magnetometer (FGM) (Russell et al. 2016) and the Search-Coil Magnetometer (SCM) (Le Contel et al. 2016), the electric field data from the Electric Double Probe (EDP) (Ergun et al. 2016; Lindqvist et al. 2016), and the 3D particle velocity distribution functions and the plasma moments from the Fast Plasma Investigation (FPI) (Pollock et al. 2016).

2. MMS Observations

Figure 1 presents one example of an electron vortex magnetic hole in the magnetosheath. The local boundary normal coordinates (LMN) determined by minimum variance analysis (MVA) of the magnetic fields (Sonnerup and Scheible, 1998) were used. In this coordinate system, **L** is the maximum variation direction that can be considered as the axis of the magnetic hole, **M** is the intermediate variation direction, and **N** is the minimum variation direction. Magnetic field strength depression from ~ 19 nT to ~ 12 nT (Figure 1a) with small field shear angle (<15°) implies that a magnetic hole is detected by MMS. The electron density (Figure 1e) and electron temperature (Figure 1d) increase while the electron parallel temperature decreases (Figure 1d) and the electron perpendicular temperature strongly increases inside the magnetic hole (Figure 1h). Here, parallel and perpendicular directions are with respect to the ambient magnetic field. There is a clear bipolar signature (from positive to negative) in V_{eN} component (Figure 1c) and a strong enhancement in electron perpendicular temperature (Figure 1d) inside the magnetic hole, which are typical features of an electron vortex (Haynes et al. 2015; Huang et al. 2017a, 2017b). The estimated width of magnetic hole (based on the frozen-in assumption) is about 27 km (0.15 ρ_i or ~ 19 ρ_e, where ρ_i ~ 175 km and ρ_e ~ 1.4 km are the proton and electron gyroradius with $|B|$ ~ 24 nT, n ~ 9 cm^{-3}, T_i ~ 850 eV and T_e ~ 100 eV). Thus, MMS detected clearly an electron-scale electron vortex magnetic hole in the magnetosheath.

Figure 2 illustrates the statistical results of electron temperature for all electron vortex magnetic holes (66 in total) in the turbulent magnetosheath from September 2015 to January 2016 (Huang et al. 2017b). It shows that the electron perpendicular temperature significantly increases inside the magnetic holes ($T_{e\perp(inside)}$ /$T_{e\perp(outside)}$ >1) for all events (Figure 2a), while the electron parallel temperature decreases ($T_{e\parallel\ (inside)}$ /$T_{e\parallel\ (outside)}$ < 1) for most of the events (Figure 2b), with a net increase in electron total temperature inside the magnetic holes for most of the events (~93%, Figure 2c). The increase of electron temperature indicates that these magnetic holes have strong correlation with the heating of electrons. The statistics of the ratio of $T_{e\perp}/T_{e\parallel}$ inside the magnetic holes (Figure 2d) show strong electron temperature anisotropies (up to 1.7) in the electron vortex magnetic holes for ~90% events. Such electron temperature anisotropy is favorable to the excitation of high frequency waves inside the magnetic holes.

After surveying the wave observations for all magnetic holes, we successfully identified the whistler waves inside 11 (17%) electron vortex magnetic holes. Figure 3 shows an example of such identification. Magnetic field strength, the ratio of $T_{e\perp}/T_{e\parallel}$, and high-pass filtered magnetic field fluctuations with cut-off frequency of 60 Hz are presented in Figure 3a-3c respectively. The occurrence of strong electron temperature anisotropy ($T_{e\perp}/T_{e\parallel}$) inside the magnetic hole is accompanied by large-amplitude magnetic fluctuations (up to 0.1 nT). Figures 3d-3h show the power spectral densities and the properties of wave emissions derived from singular value decomposition (SVD) method (Santolik et al. 2003) during this period. Intense electromagnetic waves (red or yellow in Figure 3d-3e) are observed inside the magnetic hole with their frequencies between $0.1f_{ce}$ and $0.5f_{ce}$, which corresponds to the frequency band where large-amplitude magnetic fluctuations are observed (Figure 3c). These waves have large polarization degree (>0.9 in Figure 3h) and positive ellipticity (close 1 as shown in Figure 3f), and relatively small propagation angles (<30° in Figure 3g). All these wave properties indicate that the observed fluctuations are carried out by right-hand polarized and quasi-parallel propagating whistler mode. This scenario is confirmed using the theoretical results of the linear solver of the Maxwell-Vlasov equations (WHAMP, Ronmark, 1982) shown in Figure 4. The linear dispersion relations were obtained using the local plasma parameters ($|B| \sim 12$ nT, $n \sim 10$ cm^{-3}, $T_i \sim 800$ eV and $T_e \sim 100$ eV, $T_{e\perp}/T_{e\parallel} = 1.4$). One can see a positive growth rate corresponding to $\omega/\omega_{ce} = 0.07 \sim 0.34$ due to the electron temperature anisotropy, with maximum growth rate $\gamma/\omega_{ce} = 0.04$ occurring at $\omega/\omega_{ce} = 0.23$, which is very close to ~ 0.29 ω/ω_{ce} of the peak frequency of largest power spectral densities from our observations (see in Figure 3d-3e). These theoretical results imply that the whistler waves inside the electron-scale magnetic holes can be locally generated by electron temperature anisotropy.

3. Discussions and Conclusions

The simultaneous occurrence of high frequency whistler waves and ion-scale magnetic structures (characterized by a magnetic field strength depression) was reported in the plasma sheet (Tenerani et al. 2013), but the generation mechanism of the whistler waves was not addressed in that work. Intense lion roars were often observed in mirror structures with scale-size (much/several times) larger than the ion larmor scale in the magnetosheath (Smith and Tsurutani, 1976; Thore and Tsurutani, 1981; Breuillard et al. 2017). Masood et al. (2006) have shown that some instances of lion roars could be locally generated, while the source of others must be in remote regions of the magnetosheath. Recently, a new type of electron-scale coherent structures, referred to as electron vortex magnetic hole, was identified in the turbulent magnetosheath plasma (Huang et al. 2017a, 2017b; Yao et al. 2017). The present statistical study showed an increase in electron temperature inside those magnetic holes (Figure 2), indicating that the latter may be able to heat electrons. While the mechanism of such heating remains to be elucidated, the present observations provide nevertheless a new possible way of (coherent) heating of electrons in turbulent plasmas. This mechanism can be complementary to those already proposed to explain energy dissipation at electron scales in solar wind turbulence (e.g., Sahraoui et al. 2009). Our results show furthermore that the subsequent electron temperature anisotropy instability can give rise to intense high frequency fluctuations identified as quasi-parallel propagating whistler waves, which, in turn, may accelerate electrons. Indeed, whistler waves were proposed to generate energetic electrons in the direction parallel to the ambient magnetic field through pitch-angle scattering (e.g., Kennel and Petschek, 1966). They were also shown to lead to the formation of both halo and strahl electrons in the solar wind, which could explain the generation of gamma ray bursts in interplanetary space (Vocks et al. 2005). The first evidence of simultaneous occurrence of electron-scale whistler waves and electron-scale coherent structures (i.e. electron vortex magnetic holes) reported here would help to better understand electron-scale dynamics in the magnetosheath and in other distant turbulent plasmas.

Acknowledgement

We thank the entire MMS team and instrument leaders for data access and support. This work was supported by the National Natural Science Foundation of China (41674161, 41404132, 41374168, and 41331070), and China Postdoctoral Science Foundation Funded Project (2015T80830). The French participation in the MMS mission was funded by CNES. Data is publicly available from the MMS Science Data Center at http://lasp.colorado.edu/mms/sdc/.

References

Breuillard, H. Zaliznyak, Y. Krasnoselskikh, V. Agapitov, et al. 2012 Ann. Geophys. 30, 1223-1233, https://doi.org/10.5194/angeo-30-1223-2012.

Breuillard, H. Agapitov, O. Artemyev, A. Krasnoselskikh, et al. 2014 Ann. Geophys. 32, 1477-1485, https://doi.org/10.5194/angeo-32-1477-2014

Breuillard, H., E. Yordanova, A. Vaivads, et al. 2016a, Astrophys. J., 829, 54

Breuillard, H. et al. 2016b Geophys. Res. Lett. 43, 7279–7286, doi:10.1002/2016GL069188.

Breuillard, H. et al. 2017 J. Geophys. Res. Space Physics, under review.

Cao, D. et al. 2017 Geophys. Res. Lett., 44, 3954–3962

Deng, X. M. Ashour- Abdalla, M. Zhou, R. Walker, et al. 2010 J. Geophys. Res. 115, A09225

Gary, S. P. and Madland, C. D. 1985 J. Geophys. Res. 90 (A8), 7607–7610

Ergun, R. E. et al. 2016 *Space Science Reviews*, *199*(1), 167–188

Fu, H. S. J. B. Cao, F. S. Mozer, et al. 2012 *J. Geophys. Res. 117*, A01203

Fu, H. S. et al. 2014 *J. Geophys. Res. Space Physics*, *119*, 9089–9100

Fu, H. S. A. Vaivads, Y. V. Khotyaintsev, M. André, et al. 2017 *Geophys. Res. Lett. 44*, 37–43, doi:10.1002/2016GL071787.

Fujimoto, K. 2014 Geophys. Res. Lett. 41, 2721–2728, doi:10.1002/2014GL059893.

Haynes, C. T. D. Burgess, E. Camporeale, and T. Sundberg 2015 Phys. Plasmas, 22, 012309, doi:10.1063/1.4906356.

Horbury, T. S. E. A. Lucek, A. Balogh, I. Dandouras et al. 2004 J. Geophys. Res. 109, A09209, doi:10.1029/2003JA010237.

Huang, S. Y. et al. 2010 J. Geophys. Res. 115, A12211, doi:10.1029/2010JA015335.

Huang, S. Y. et al. 2012a Geophys. Res. Lett. 39, L11104, doi:10.1029/2012 GL052210.

Huang, S. Y. M. Zhou, X. H. Deng, Z. G. Yuan et al. 2012b Ann. Geophys. 30, 97–107, doi:10.5194/angeo-30-97-2012.

Huang, S. Y. F. Sahraoui, X. H. Deng, J. S. He et al 2014 Astrophys. J. Lett.789, L28, doi:10.1088/2041-8205/789/2/L28.

Huang, S. Y. et al. 2016a J. Geophys. Res. Space Physics, 121, 6639–6646

Huang, S. Y. et al. 2016b Geophys. Res. Lett. 43, 7850–7858, doi:10.1002/2016GL070033.

Huang, S. Y. et al. 2017a Astrophys. J. Lett. 836, L27, doi:10.3847/20418213/aa5f50.

Huang, S. Y. et al. 2017b J. Geophys. Res. Space Physics, 122, 8577–8588

Huang, S. Y. et al. 2017c J. Geophys. Res. Space Physics, 122, 7188–7196

Huang, S. Y. L. Z. Hadid, F. Sahraoui, Z. G. Yuan et al. 2017d Astrophys. J. Lett. 836, L10, doi.org/10.3847/2041-8213/836/1/L10

Kennel, C. F., and H. E. Petschek, 1966 J. Geophys. Res., 71(1), 1–28

Lacombe, C., Alexandrova, O. Matteini, L. Santolik, O. et al. 2014 Astrophys. J. 796, 5. doi:10.1088/0004-637X/796/1/5

Le Contel, O. et al. 2009 Ann. Geophys. 27, 2259–2275, doi:10.5194/angeo-27-2259-2009.

Le Contel, O. et al. 2016 Space Sci. Rev. 199(1), 257–282, doi:10.1007/s11214-014-0096-9.

Li, H. M. Zhou, X. Deng, Z. Yuan, et al. 2015 J. Geophys. Res. Space Physics, 120, 1086–1095, doi:10.1002/2014JA020474.

Li, W. J. Bortnik, R. M. Thorne, Y. Nishimura et al. 2011 J. Geophys. Res. 116, A06206, doi:10.1029/2010JA016313.

Lindqvist, P.-A. et al. 2016 Space Sci. Rev. 199, 137–165, doi:10.1007/ s11214-014-0116-9.

Masood, W. S. J. Schwartz, M. Maksimovic, and A. N. Fazakerley 2006 Ann. Geophys. 24, 1725– 1735, doi:10.5194/angeo-24-1725-2006.

Moullard, O. A. Masson, H. Laakso, M. Parrot et al. 2002 Geophys. Res. Lett. 29(20), 1975, doi:10.1029/2002GL015101.

Pollock, C. et al. 2016 Space Sci. Rev. 199, 331–406, doi:10.1007/s11214-016-0245-4.

Rönnmark, K. 1982, Computation of the dielectric tensor of a Maxwellian plasma, Tech. rep.

Russell, C. T. et al. 2016 Space Sci. Rev. 199, 189–256, doi:10.1007/s11214-014-0057-3.

Santolik O. M. Parrot, and F. Lefeuvre 2003 Radio Sci. 38 (1), 1010

Santolık, O. M. Parrot, U. S. Inan, D. Buresova et al. 2009 J. Geophys. Res. 114, A03212, doi:10.1029/2008JA013776.

Sahraoui, F., Belmont, G., Pin¸con, J., et al. 2004, AnGeo, 22, 2283

Sahraoui, F. G. Belmont, L. Rezeau, and N. Cornilleau-Wehrlin 2006 Phys. Rev. Lett. 96, 075002.

Sahraoui, F., Goldstein, M. L., Robert, P., & Khotyaintsev, Y. V. 2009, PhRvL, 102, 231102

Shi, Q. Q. et al. 2009 J. Geophys. Res. 114, A10202, doi:10.1029/2009JA014283.

Stasiewicz, K. 2004 Phys. Rev. Lett. 93, 125,004, doi:10.1103/ PhysRevLett.93.125004.

Stenzel, R. L. 1999 J. Geophys. Res. 104(A7), 14379–14395, doi:10.1029/1998JA900120.

Sonnerup, B. U. O. and M. Scheible, Minimum and maximum variance analysis, in Analysis methods for Multi-spacecraft data, edited by G. Paschmann and P. W. Daly, no. SR-001 in ISSI

Scientific Reports, Chap. 1, pp. 185-220, ESA Publ. Div. Noordwijk, Netherlands, 1998.

Smith, R. L. 1961 J. Geophys. Res. 66, 3699–3707, doi:10.1029/JZ066i011p03699.

Streltsov, A. V. M. Lampe, W. Manheimer, G. Ganguli et al. 2006 J. Geophys. Res. 111, A03216, doi:10.1029/2005JA011357.

Sundberg, T., Burgess, D., & Haynes, C. T. 2015, JGRA, 120, 2600

Tenerani, A. et al. 2012 Phys. Rev. Lett. 109, 155,005.

Tenerani, A. O. Le Contel, F. Califano, P. Robert et al. 2013 J. Geophys. Res. Space Physics, 118, doi:10.1002/jgra.50562.

Tsurutani, B. T. B. Dasgupta, C. Galvan, M. Neugebauer et al. 2002 Geophys. Res. Lett. 29(24), 2233, doi:10.1029/2002GL015652.

Thorne, R. M. and B. T. Tsurutani 1981 *Nature*, *293*, 384–386, doi:10.1038/293384a0.

Vocks, C., Salem, C., Lin, R. P., & Mann, G. 2005, ApJ, 627, 540

Xia, Z. L. Chen, L. Dai, S. G. Claudepierre, et al. 2016 Geophys. Res. Lett. 43, 9444–9452, doi:10.1002/2016GL070280.

Yao, S. T. et al. 2017 J. Geophys. Res. Space Physics, 122, doi:10.1002/2016JA023858.

Zhima, Z. J. Cao, H. Fu, W. Liu 2015 et al. J. Geophys. Res. Space Physics, 120, doi:10.1002/2014JA020786.

Zhang, Y. H. Matsumoto, and H. Kojima 1999 J. Geophys. Res. 104(A12),28633–28644, doi:10.1029/1999JA900301.

Figure Captions

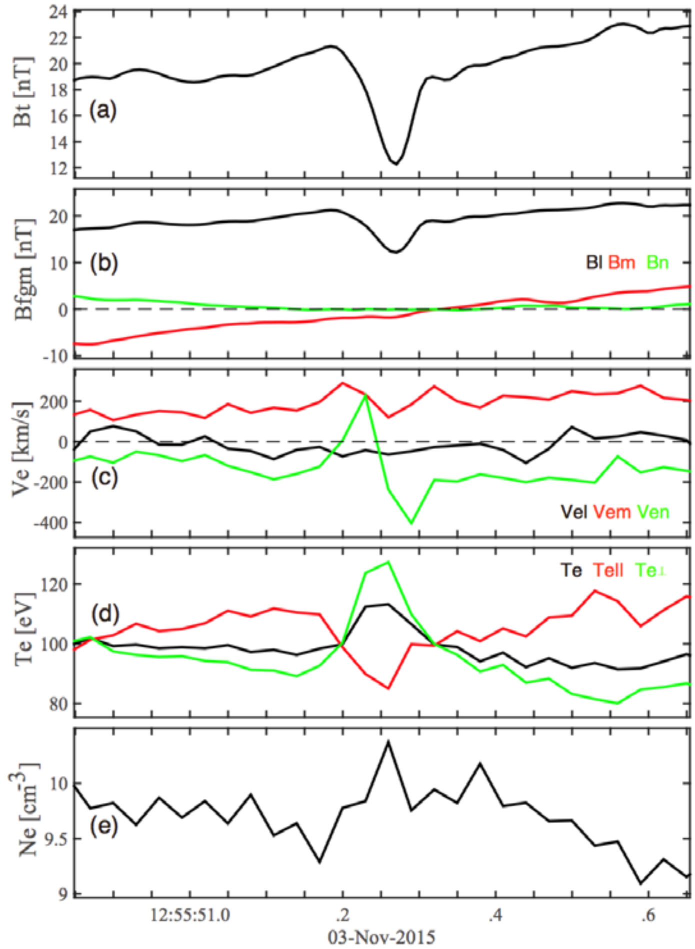

Figure 1. Example of electron-scale electron vortex magnetic hole observed on Nov 03 2015 in the magnetosheath. (a) Magnetic field strength; (b) Three components of magnetic field in LMN coordinates; (c) Three components of electron velocity in the LMN coordinates; (d) Electron temperature (black), parallel temperature (red) and perpendicular temperature (green); and (e) Electron density.

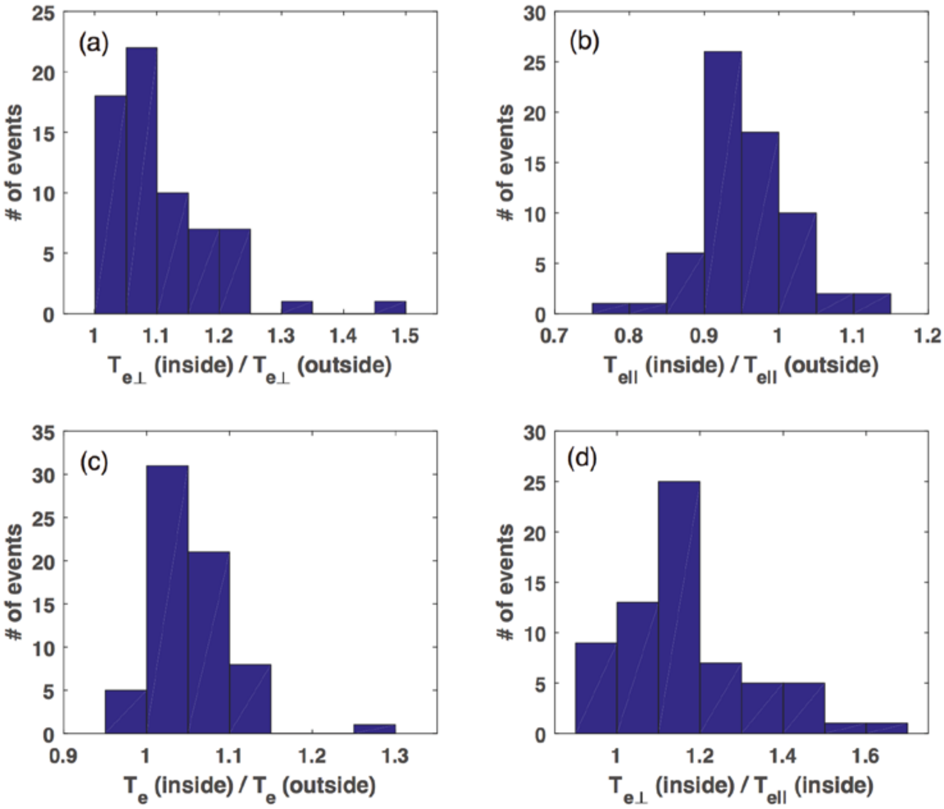

Figure 2. Electron temperatures inside the electron vortex magnetic holes and outside these magnetic holes observed by MMS from September 2015 to January 2016. The ratios of (a) perpendicular temperatures, (b) parallel temperatures and (c) total temperatures inside the holes to these outside the holes; (d) the ratios of perpendicular temperatures to parallel temperature inside the holes.

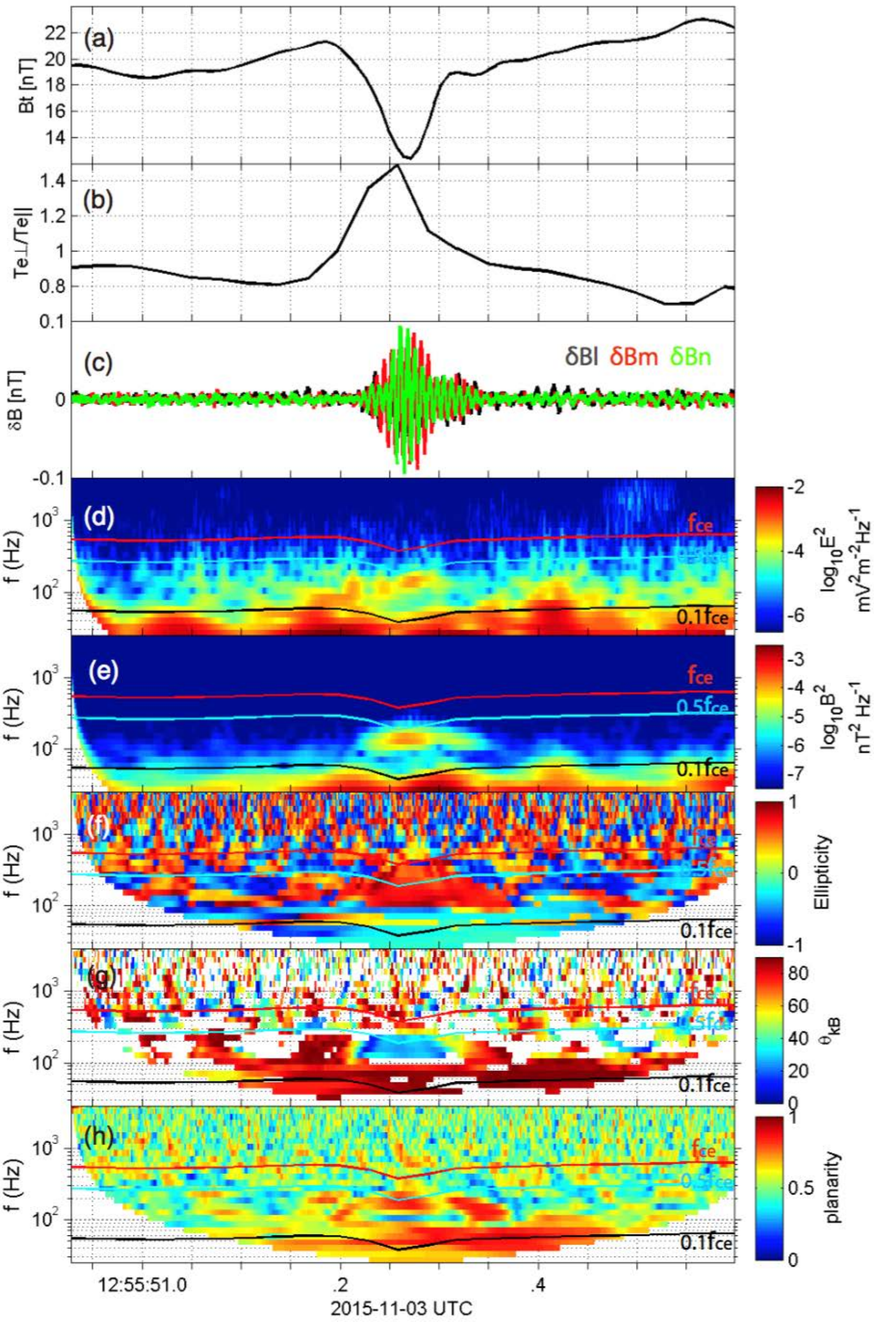

Figure 3. Example of the observations of whistler waves inside electron vortex magnetic holes on 03 November 2015. (a) Magnetic field strength; (b) The ratios between electron perpendicular temperature and parallel temperature; (c) Filtered magnetic field fluctuations from SCM instruments; (d)-(e) Power spectra densities of the electric and magnetic components of the waves; (f) Ellipticity (positive or red: right hand polarization; negative or blue: left hand polarization); (g) Propagation angle; (h) Polarization degree. The black, cyan, red curves in (d-h) indicate the frequencies 0.1 f_{ce}, 0.5 f_{ce}, and 1.0 f_{ce}, respectively.

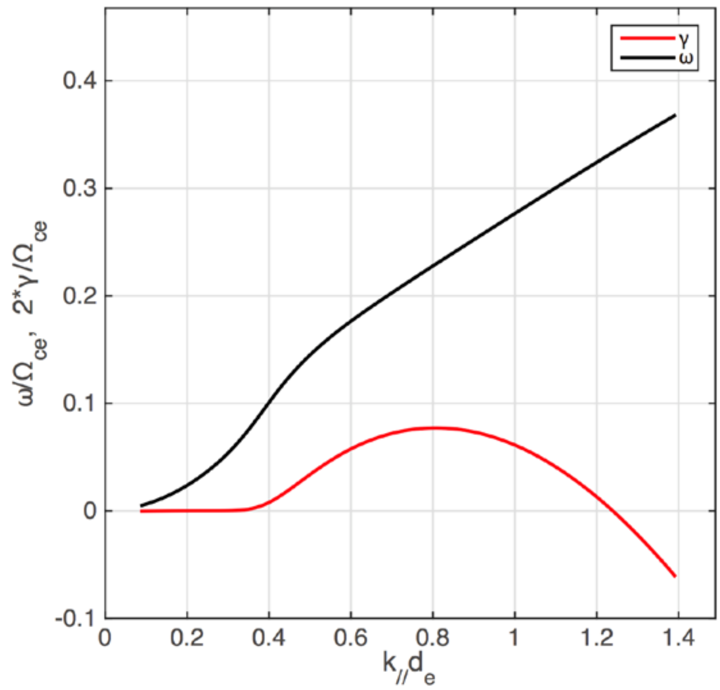

Figure 4. The dispersion relations (black) and growth rates (red) of the theoretical whistlers based on the plasma parameters from local observations inside the electron vortex magnetic hole. The local plasma parameters used to calculate the growth rate of whistler waves: $|B|$ ~ 12 nT, n ~ 10 cm^{-3}, T_i ~ 800 eV and T_e ~ 100 eV, $T_{e\perp}/T_{e\parallel} = 1.4$.